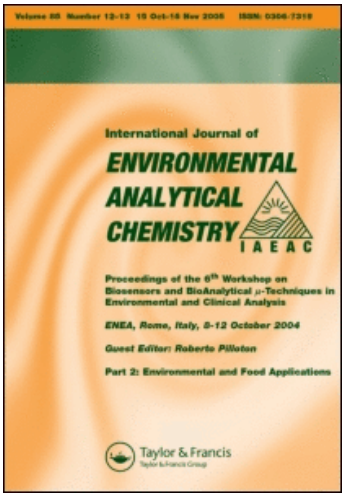

International Journal of Environmental Analytical Chemistry

Publication details, including instructions for authors and subscription information:
http://www.informaworld.com/smpp/title~content=t713640455

A submersible immunosensor

Rebecca A. Fisher[a]; Scott J. Melton[a]; Diane A. Blake[ab]
[a] Department of Biochemistry, Tulane University, School of Medicine, SL-43, New Orleans, LA 70112, USA [b] Tulane/Xavier Center for Bioenvironmental Research, New Orleans, LA, USA

Online publication date: 20 January 2011

To cite this Article Fisher, Rebecca A. , Melton, Scott J. and Blake, Diane A.(2011) 'A submersible immunosensor', International Journal of Environmental Analytical Chemistry, 91: 2, 123 — 137
To link to this Article: DOI: 10.1080/03067311003628653
URL: http://dx.doi.org/10.1080/03067311003628653

Intern. J. Environ. Anal. Chem.
Vol. 91, No. 2, 15 February 2011, 123–137

Taylor & Francis
Taylor & Francis Group

A submersible immunosensor

Rebecca A. Fisher[a], Scott J. Melton[a] and Diane A. Blake[ab]*

[a]*Department of Biochemistry, Tulane University, School of Medicine, 1430 Tulane Avenue, SL-43, New Orleans, LA 70112, USA;* [b]*Tulane/Xavier Center for Bioenvironmental Research, New Orleans, LA, USA*

(*Received 24 August 2009; final version received 15 January 2010*)

A prototype submersible immunosensor with autonomous sampling characteristics has been designed and fabricated in conjunction with Sapidyne Instruments Inc. The watertight instrument is battery-powered and internally controlled; the internal controller can interface with an external computer for modification of the experimental parameters and review of results. An environmental sample is collected from the external space via a motor driven syringe such that displacement of the motor arm corresponds to a specific intake volume. Assay reagents, buffer and fluorescently labelled antibody, stored in bags within the sensor, are drawn into the syringe after the environmental sample and mixed. The final solution containing the environmental analyte and labelled antibody then passes over a flow/observation cell containing rigid 98-micron beads coated with the analyte of interest. The sensor continuously monitors the fluorescence across the flow cell and the difference in signal from the beginning to the end of the run can be converted to an estimate of analyte concentration. After optimisation steps that included selection of the fluorophore and bead support, the sensor could mix preloaded reagents and autonomously develop a standard curve for two different analytes: caffeine, a marker for untreated sewage, and hexavalent uranium, which contaminates the groundwater in the vicinity of uranium mining and processing sites. The coefficient of variation was near 15% for all concentrations examined. The minimum levels of detection for caffeine and hexavalent uranium in this assay system were 60 and 241 pM, respectively. Spike and recovery assays showed that the sensor was able to accurately predict the concentration of both analytes within the linear region of the calibration curve. Analysis of real environmental samples contaminated with uranium showed good agreement between the sensor and a standard analytical method, thus demonstrating the suitability and versatility of the submersible immunosensor as a field instrument.

Keywords: immunosensor; flow fluorimeter; monoclonal antibodies; caffeine; uranium; autonomous underwater sensor

1. Introduction

The capability to monitor environmental water quality in large bodies of water is important under a variety of conditions, including environmental remediation, food safety and emergency responses. In this era of increased environmental awareness and responsibility, the remediation of known sites of contamination, especially from sources such as nuclear waste or munitions manufacture, has become a priority [1]. Food safety is

*Corresponding author. Email: blake@tulane.edu

ISSN 0306–7319 print/ISSN 1029–0397 online

DOI: 10.1080/03067311003628653
http://www.informaworld.com

a concern in consumption of wild-caught shellfish and certain species of fin fish; every year people become ill or die from eating seafood contaminated with toxins produced by harmful algal blooms [2]. Emergency response teams, whether dealing with an industrial accident or a national security threat, need to know both the identity and the level of contaminants in a suspect body of water to keep the public, and themselves, safe [3].

The development of biosensors, which use a biological component to assay for a contaminant, is a promising area for water monitoring. The most common sensing molecules for aquatic samples include nucleic acids, whole cells, enzymes and antibodies. A large number of biosensors based on nucleic acids have been able to detect toxic algae species [4–6] and microorganisms [7,8] using probes that hybridise to sequences unique to the target. While these biosensors are able to recognise targets present in low quantities with a high degree of specificity, the nucleic acid extractions required for these biosensors require laboratory facilities that are not usually available in the field. Work is currently progressing on techniques to simplify nucleic acid extraction that could be coupled to field based sensors [9]. Recently the use of nucleic acid aptamers in biosensors has shown promise with a wide variety of target analytes (for reviews see [10,11]). However, their use in aquatic environments or water quality monitoring has thus far been limited. Problems with this approach include cross reaction with other targets when analysing metal ions [12], and use of non-portable laboratory-based equipment such as spectrophotometers [13] and surface plasmon resonance instruments [14] for detection methods. Techniques using dipsticks or lateral flow sensors with a colorimetric readout, which are better suited to field applications, are also being researched [15].

Whole cell sensor systems for use in aquatic environmental monitoring are usually based on living algae or bacteria. These sensors are most often used to determine the overall toxicity in a water sample [16,17]; in some cases, assay systems have been developed to identify a broad class of toxins such as pesticides [18]. Whole cell systems that distinguish individual contaminants often rely on genetically engineered strains of bacteria [19,20], and may lack sensitivity [21]. When using whole cells for sensing, cellular viability can also be a confounding variable.

Enzymatic biosensors used in aquatic environments are often coupled to electrochemical detection methods. Target contaminants are generally organic molecules that can be acted upon by naturally occurring enzymes [22–25]. Immobilising the enzyme while preserving catalytic activity has remained a major hurdle in development of these sensors and alternate methods for utilising enzymatic potentials are under development (see [26] for a review). As in the whole cell systems, genetic engineering of enzymes is a current approach for enhancing sensor properties [27].

Immunosensors, which are functionalised with antibodies, have a very broad range of target applications including toxins [28], bacteria [29–31], pesticides [32–34] and inorganic molecules [35,36]. Antibodies against novel targets must be produced from immunised animals, screened, purified and characterised. However, once this process has been completed, antibodies offer several characteristics that can make them preferable to the other biosensor sensing molecules; these include high degrees of specificity, stability and functionality. Antibodies display a very high degree of specificity for the target selected; with proper selection strategies and/or combinatorial reengineering, cross reactivity with similarly structured molecules can be minimised. Purified antibodies show quite acceptable stability and can be used for the analysis of a wide variety of samples. Additionally, antibodies are easily functionalised on many surfaces in contrast to enzymatic biosensors,

which require the enzyme to be very carefully captured within membranes or otherwise immobilised without loss of activity.

Most current biosensor designs, however, have the same major limitation; they require humans to enter into the toxic environment to gather samples. Here we present a novel prototype underwater immunosensor that can be deployed with an unmanned submersible vehicle. The sensor was designed to autonomously sample the external aqueous environment and analyse it for the contaminant of choice. This will allow information to be gathered and analysed quickly and efficiently in situations where it may be inadvisable to send a human, such as in a mass casualty incident or military operation. Such a sensor could also be useful when it is necessary to sample large areas, such as a large harmful algal bloom or industrial spill. Instead of spending several days drawing samples from different depths and different locations and still more time analysing them, the underwater sensor described herein could travel around a target area, taking samples and analysing them while still in the field.

The research presented herein describes the process of laboratory validation and optimisation of the sensor for the detection of two different analytes. Caffeine has been advocated for use as a chemical indicator of anthropomorphic inputs into marine ecosystems due to its presence in untreated wastewater [37–39]. Caffeine is also being evaluated as a marker for assessing water pollution caused by human activities [40,41]. To further demonstrate the versatility of the instrument, the sensor was also adapted for the detection of hexavalent uranium. Uranium, as a radioactive heavy metal, is a persistent environmental contaminant at uranium mining and processing sites, and there is much interest in its detection and remediation in groundwater sources [42–44].

2. Experimental

2.1 *Materials*

The uranium-selective chelator, 2,9-dicarboxyl-1,10-phenanthroline (DCP) was purchased from Alfa Aesar (Ward Hill, MA). The monoclonal anti-caffeine antibody (clone 9401) was a product of Biodesign (Saco, ME). The caffeine-bovine serum albumin conjugate (caffeine-BSA) used for immobilisation on the bead support was purchased from YJ Bio-Products (Rancho Cordova, CA). Chelated uranium covalently conjugated to bovine serum albumin (U(VI)-DCP-BSA) was available from a previous study [45]. Polystyrene and polymethylmethacrylate beads (98 μm diameter), disposable flow cells and mesh filter supports were from Sapidyne Instruments, Inc (Boise, ID). Caffeine, bovine serum albumin (BSA), and buffer salts to make phosphate buffered saline (PBS, 137 mM NaCl, 3 mM KCl, 10 mM phosphate, pH 7.4) and HEPES buffered saline (HBS, 137 mM NaCl, 3 mM KCl, 10 mM HEPES, pH 7.4) were purchased from Sigma-Aldrich (St. Louis, MO). PBS was used for all experiments with caffeine; HBS was used for all experiments with uranium. Goat anti-mouse IgG Fab secondary antibody labelled with DyLight 649 was purchased from Jackson ImmunoResearch Laboratories (West Grove, PA).

2.2 *Immobilisation of capture ligand on bead support and filling of flow cells*

The caffeine-BSA or U(VI)-DCP-BSA was diluted to a final concentration of 20 μg in 1.0 mL of PBS or HBS. An aliquot (200 mg dry weight) of the bead support (polystyrene or polymethylmethacrylate) was then added and the mixture was mixed on a rotating plate

for either 1 hour at 37°C or overnight at 4°C to allow surface adsorption of the conjugate to the beads. The conjugate solution was removed and the beads were washed once with 1.0 mL of PBS or HBS. To prevent nonspecific binding of the antibody, 1.0 mL of a 30 mg mL^{-1} BSA solution in PBS or HBS was added to the beads and the mixture was allowed to incubate at room temperature on a rotating plate for 1 hour. Before use, the beads in blocking solution were added to 30 mL of PBS or HBS to bring the concentration of beads to 6.67 mg mL^{-1}. The blocked beads were then packed into disposable flow cells that could subsequently be installed in the sensor. A mesh filter support (4 mm diameter) was added to the bottom of each flow cell to support the beads. Although the flow cells could be packed manually, cell-to-cell reproducibility was improved when the flow cells were packed automatically using a program written for the KinExA 3000^{TM} Instrument (Sapidyne Instruments, Boise, ID) also available in the laboratory. A flow cell containing the bottom filter was installed in the KinExA 3000^{TM} and the diluted bead suspension was added to the bead vial of this instrument. The instrument was then programmed to draw 4.750 mL of bead suspension (31.7 mg of beads) from the bead vial and push that over the flow cell to fill it. The flow cell was then detached from the KinExA 3000^{TM} and a second mesh filter was added to the top of the packed beads to stabilise the capture reagent. Each 200 mg aliquot of coated beads was sufficient to pack 6 flow cells. Packed flow cells could be stored submerged in PBS or HBS containing 0.03% NaN_3 at 4°C for at least 2 weeks without significant loss of signal. A picture of the packed flow cell is shown in Figure 1.

2.3 *Fluorescent labelling of monoclonal antibodies*

The anti-caffeine antibody was fluorescently labelled using two different kits: the Amersham Cy5 Ab Labeling Kit from GE Healthcare (Piscataway, NJ) and the DyLight 649 Labeling Kit from Pierce Biotechnology (Rockford, IL). The kit instructions were followed exactly as written using the 9401 monoclonal anti-caffeine antibody.

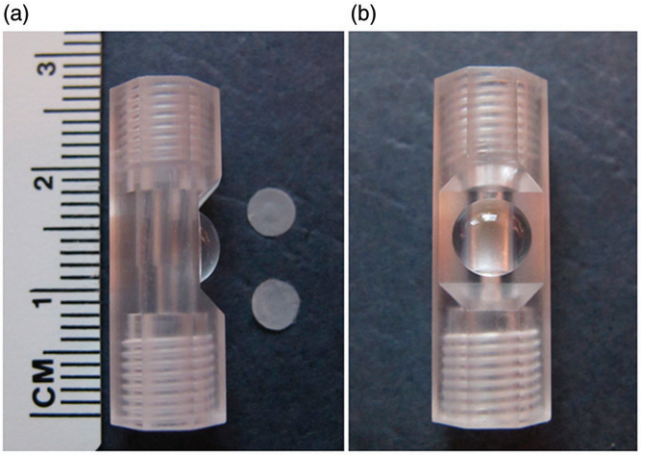

Figure 1. Flow cell for the underwater sensor; (a) Side view of sensor flow cell, showing threaded connections, the semicircular lens that directs light to the detector of the instrument, and the filters installed to stabilise the beads in the flow cell. Centimetre rule included for scale; (b) Front view of a flow cell packed with 98 μm diameter beads.

The fluorophores used in the two kits were different but were both NHS-ester conjugates that reacted with primary amine groups (primarily lysine side chains) on the antibody. The anti-uranium antibody used in this study, 12F6, was inactivated when its lysine residues were chemically modified (unpublished data); this antibody was non-covalently labelled by the addition of a 10-fold molar excess of goat anti-mouse IgG Fab secondary antibody labelled with DyLight 649.

2.4 *Sensor features and experimental setup*

The underwater immunosensor was constructed by Sapidyne Instruments (Boise, ID) in an academic-industrial partnership that has been used to successfully develop other sensor systems for environmental analysis [35–36,46]. The optical unit used in this device is identical to that in a previously described In-line sensor [35–36,46]. Details of the kinetic exclusion method are also described in previous publications [47–49].

2.4.1 *Sensor flow connections*

One of the distinguishing features of the underwater sensor is its ability to autonomously collect samples from an aqueous environment and analyse them. For some applications, the sensor must be able to construct a calibration curve from reagents contained in the case. Figure 2 shows a diagram of all the plumbing connections in the sensor. Lines 1–6 carry standards for the analyte of interest used to construct a calibration curve; these lines are integrated into the main flow path to the draw syringe via valve 1. Secondary reagents such as buffer, labelled antibody, and the external sample are processed through valve 2. Additionally, valve 2 provides the outlet for the mixing compartment and a connection to

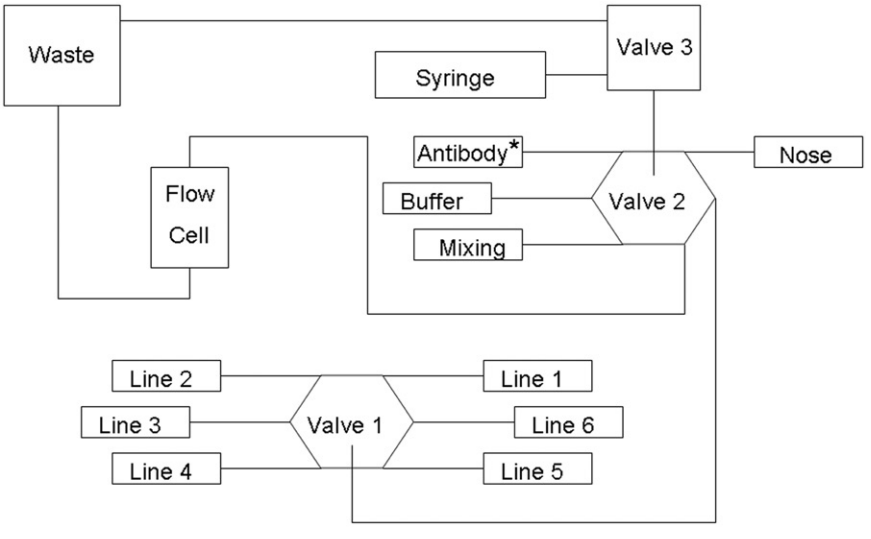

Figure 2. Flow connections for the underwater sensor. Lines 1–6 contain standards of known concentration, while the nose line is the inlet for the environmental sample. The Antibody* compartment holds the fluorescently labelled antibody. All solutions are drawn into the syringe and sent over the flow cell after combining with the antibody in the mixing compartment.

valve 1 or the flow cell. The last valve, valve 3, is only connected to the draw syringe and the waste line.

A description of the flow path for the analysis of standards follows. It may be helpful to refer back to Figure 2 as the movement of the standard through the sensor is detailed. First, the standard must be drawn into the syringe, taking it through valves 1, 2, and 3 in that order. Labelled antibody is added to the standard already in the syringe through valves 2 and 3. The next destination is the mixing compartment; the standard must pass back through valves 3 and 2 to reach it. This volume is then pushed back and forth between the mixing compartment and the draw syringe through both valves to facilitate mixing. Upon completion of mixing, the standard is retained in the draw syringe, ready for analysis. To reach the flow cell the standard must once again pass through valves 3 and 2. Then the standard travels through the bead pack in the flow cell, and is finally collected as waste.

2.4.2 *Sensor anatomy*

Since the sensor is designed for underwater use, it has several unique features adapted for this environment. Figure 3 shows photographs of the most important sensor features. Anytime electronics are to be used in an environment where liquid is present, a waterproof shield or case is warranted. This is especially important as increasing water pressure becomes a factor. Figure 3a shows the waterproof case next to the sensor itself. The case is made from aluminum and has a waterproof gasket where the body and the cap join to keep out moisture. The sensor draws samples based on displacement of the plunger in the draw syringe, shown in Figure 3b. The optical unit is contained behind the flow cell bracket as shown in Figure 3c. In order to analyse samples underwater, reagents must be self contained inside the case. Figure 3d shows the reagent bags located at the back end of the sensor. The bags are connected via tubing to the appropriate valve to make a watertight flow path. One of the distinguishing characteristics of the sensor is the ability to draw samples from the external environment. Figure 3e is a photograph of the cap of the waterproof case showing the exterior inlet, or nose line, for drawing samples into the sensor for analysis. The nose is equipped with a filter to remove particulates, preventing clogging of the interior tubing. Power is supplied to the sensor with a rechargeable battery pack containing NiMH C-type batteries. The battery pack is located in the base of the sensor and is not visible in the photographs.

2.4.3 *Sensor operation and experimental set-up*

The sensor is a flow fluorimeter that analyses samples based on the principle of kinetic exclusion (described in [47–49]). The pattern of valve changes necessary for analysing samples is programmed into the sensor using a timing file. A laptop computer is connected to the sensor to upload the file and to retrieve data after the experiment; however, the computer does not have to be connected to the sensor to run the timing file. The underwater sensor has an accompanying program with a user-friendly interface for structuring the timing file. Each line specifies the source to be drawn/dispensed from/to (line 3, line 5, buffer, antibody label, etc.), the volume in μL to be drawn, and the rate at which the action is to be performed. Analysing a standard or unknown sample follows the same sequence of actions every time. The set-up of an experiment will be briefly outlined here. A more detailed timing file that includes volumes and rates can be viewed in the

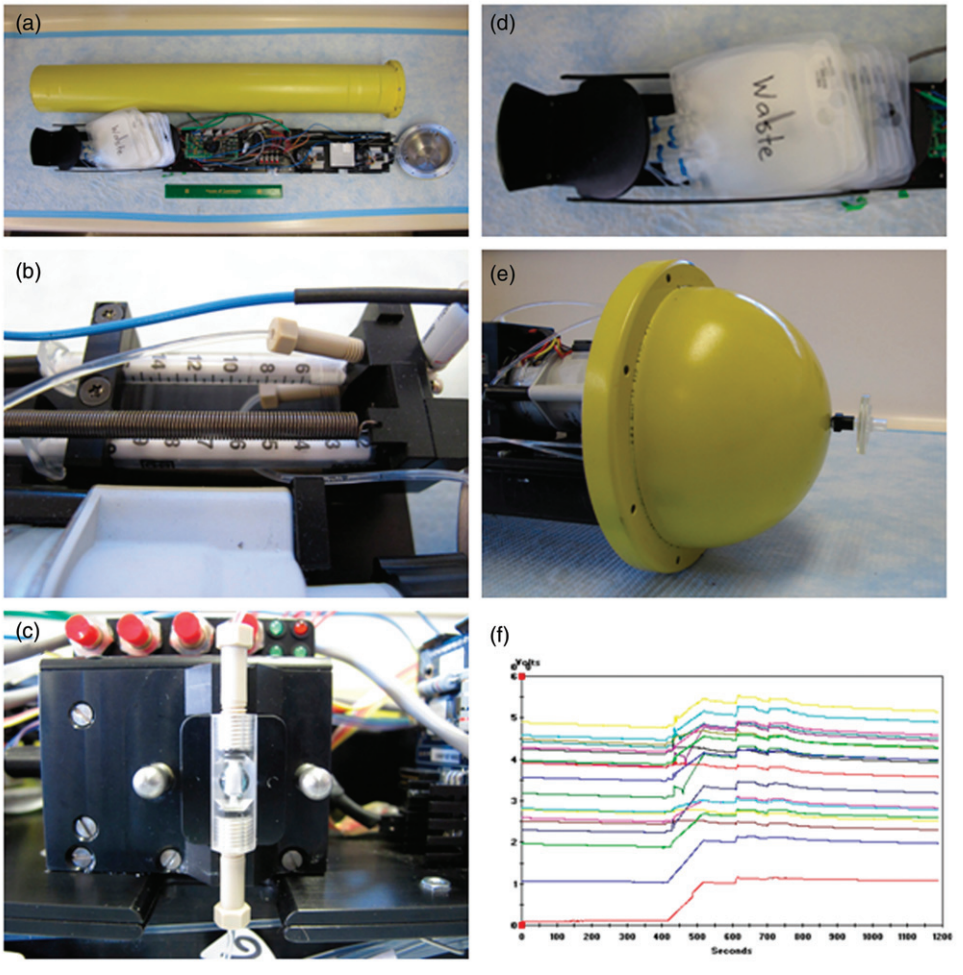

Figure 3. Features of the underwater sensor. (a) Interior view of sensor and its watertight case, with standard ruler for scale; (b) draw (top) and mix (bottom) syringes; (c) flow cell and optics unit; (d) bags for reagents and waste; (e) exterior inlet in nose for collection of environmental sample; (f) sample data traces. The average change in voltage in a five second interval at the beginning of the run is subtracted from the average voltage of a similar interval at the end of the run to give the overall difference in volts. This difference (termed delta) is a measure of the antibody free binding sites (i.e. antibody not in complex with ligand), which can be used in subsequent determinations of analyte concentration.

supplementary materials section. At the end of each experiment, all of the lines in the instrument are rinsed sequentially five times with 0.3 mL each of water, 10% household bleach, and water.

Before beginning analysis, all lines were charged with reagent. This ensured that the concentration of reagent that reached the draw syringe was not diluted by water retained in the lines after post experiment rinsing. Charging was accomplished by drawing a volume slightly greater than the volume of the lines (200 μL) and pushing that to waste. This action

was performed twice, then a standard was drawn from the reagent bag and sent to the mixing compartment, followed by the labelled antibody. Mixing consisted of passing the sample back and forth between the draw syringe and mixing compartment. After mixing was completed, the sample was passed over the flow cell containing the coated beads and fluorescence level was monitored by the optical unit. The sensor went through several rinsing steps to remove traces of the previous standard or sample before moving on to the next one. The syringe was rinsed first, followed by the flow cell and mixing compartment. The rinse cycle ended by washing out the syringe again. The analysis and the rinsing steps constituted a single run. The sensor output is a plot of the voltage over time as the sample is moving through the sensor. At the end of each run, the output is available to view, but needs to be downloaded from the sensor to a computer. A sample of the data output, consisting of 19 runs, is shown in Figure 3f. The initial baseline (0–405 sec) represents the time required for the standard or sample to be drawn and mixed with the antibody. The middle linear region (405–525 sec) occurs when the standard or sample passes over the flow cell in view of the optics unit, and the remainder of the plot (525–1190 sec) consists of the washing steps. The sensor software calculates the delta by subtracting the average voltage over a five second interval at the beginning of each run from a similar interval at the end. The change in fluorescence associated with the sample is represented by the delta value, which is used to construct standard curves and estimate unknowns. Due to the necessity of the mixing and washing steps, one run, which is the analysis of one sample, takes 20 minutes to complete. For spike and recovery experiments, the calibration curve was always constructed first; then the unknown samples were analysed.

2.5 *Caffeine detection in spiked buffer samples*

All preliminary sensor characterisation, including fluorescent label selection, evaluation of the solid support, and tests of linearity with antibody concentration, were performed using fluorescently labelled anti-caffeine antibodies and caffeine-BSA adsorbed on the solid support. For evaluation of analytical performance, the sensor autonomously prepared all assay mixtures in PBS containing 132.5 pM Dylight-649 labelled 9401 antibody, 50 $\mu g\,mL^{-1}$ BSA, and caffeine at concentrations of 0–5.0 nM.

2.6 *Uranium detection in environmental samples*

Polystyrene beads were coated with a DCP-BSA conjugate as described in Section 2.2 above. Before the beads were packed into the flow cells, they were incubated in the presence of 1 μM uranium for at least 5 minutes in order to form the U(VI)-DCP complex. These beads were then loaded into the flow cells as described above; the excess uranium was removed during the subsequent washing of the bead pack in the flow cell.

Groundwater samples contaminated with uranium were available from another project [46]. Environmental samples were acidified to pH 2 to release the U(VI) from natural chelators; subsequent dilution of each sample into assay buffer containing DCP allowed the U(VI) to form a complex with DCP. Details of this procedure are described in [46]. For the standard curve, the operator mixed the assay mixtures by adding uranium (0–10 nM) to HBS containing BSA (50 $\mu g\,mL^{-1}$), DCP (200 nM), 12F6 monoclonal antibody (0.25 nM), DyLight 649 labelled goat anti-mouse IgG Fab secondary antibody (2.5 nM) and a 1:400 dilution of artificial groundwater (described in [46]). For analysis of

environmental samples, the sensor mixed the sample such that the final dilution was 1 : 400 in HBS containing DCP (200 nM), 12F6 monoclonal antibody (0.25 nM), DyLight 649 labelled goat anti-mouse IgG Fab secondary antibody (2.5 nM) and BSA (50 $\mu g\,mL^{-1}$).

3. Results and discussion

3.1 *Fluorescent label selection*

The size and power requirements imposed on the underwater sensor preclude the use of the pumps that prepare a fresh bead pack for every sample (as in the KinExA 3000™ and In-line Sensor). Instead, the underwater sensor contained a flow cell with a large bead pack that was used to analyse multiple samples, as shown in Figure 1. The optical unit on the underwater sensor required the use of a fluorophore with excitation/emission spectra in the far red wavelengths; two commonly used fluorophores with these characteristics, Cy5 and DyLight 649, were therefore tested for suitability in this new sensor format. The ideal fluorophore for use in the sensor would provide a consistent delta signal each time a fixed concentration of fluorescently labelled antibody was passed over the flow cell. The two candidate fluorophores were therefore conjugated to the anti-caffeine monoclonal antibodies and the sensor was programmed to apply varying concentrations of the fluorescently labelled antibody to the flow cell (data not shown). Concentrations of labelled antibody that resulted in a delta value of near 0.15 were chosen for subsequent experiments. Because the sensor is only capable of reading a fluorescent signal up to approximately 15 volts, a relatively low delta value was chosen so that a large number of sequential experiments ($n = 90$) could be performed. The sensor was then programmed to sequentially inject equal aliquots of labelled antibody onto the flow cell, and the delta values were plotted for each run, as shown in Figure 4. The Cy5 labelled antibody showed a peak in delta values after ~10 runs and then the values drifted lower with every cycle,

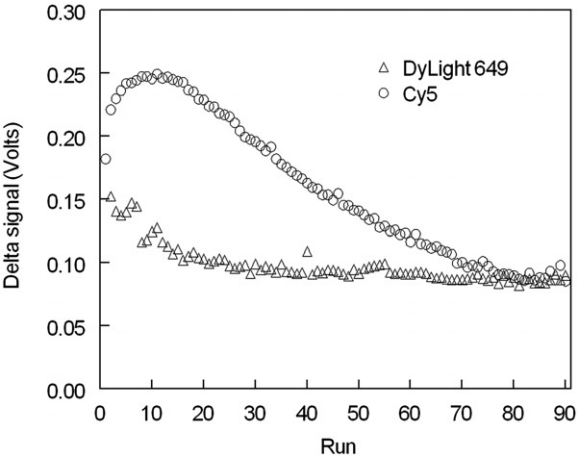

Figure 4. Effect of fluorophore on signal stability in the underwater sensor. Replicate assay mixtures ($n = 90$) containing Cy5- or Dylight 649-labelled anti-caffeine antibody were applied to a flow cell packed with beads coated with a caffeine-BSA conjugate. The signal generated from each trace was replotted versus the number of consecutive experiments performed on the flow cell.

never stabilising. The delta values ranged from 0.25 at the peak to 0.10 in the last run with an average of 0.159 volts and a coefficient of variation (CV) of 35.5%. In contrast, the DyLight 649 labelled antibody showed a plateau in delta value of just under 0.10 after 10 runs, which was maintained until the end of the experiment. The average delta value was 0.0986 volts with a CV of 15.4%. Therefore the DyLight 649 labelled anti-caffeine antibody was selected for use in this sensor because it provided a more stable signal over the life of an individual flow cell.

3.2 *Bead support selection*

The sensor uses a column of rigid 98 micron polymer beads coated with a structural analogue of the ligand being measured to capture antibody that is not complexed to ligand. Two commonly used rigid polymer bead materials, polystyrene and polymethylmethacrylate, were tested in the underwater sensor to further optimise the assay system for the caffeine model analyte. To assess the performance of the bead support, varying concentrations of the fluorescently labelled antibody were applied to a single flow cell packed with polymer beads coated with caffeine-BSA. Replicate ($n = 5$) linear dose-response curves were constructed by plotting antibody concentration versus delta signal, the slopes of the lines thus generated were averaged and the CV compared between the two bead support materials. A lower CV indicated a more stable instrument response. Figure 5 shows the linear dose response curves for each bead material. The data gathered on the polystyrene beads, shown in Panel A, displays good agreement on both the individual delta values and on the slopes of the lines generated. The average slope was 0.004406 volts/pM antibody with a CV of 13%. The polymethylmethacrylate beads, however, did not demonstrate the same degree of reproducibility, as shown in Panel B of Figure 5. Here the average slope was 0.000069 volts/pM antibody with a CV of 32%. Additionally, the delta values obtained using coated polymethylmethacrylate beads were much lower, even though a higher concentration of antibody was used to construct the

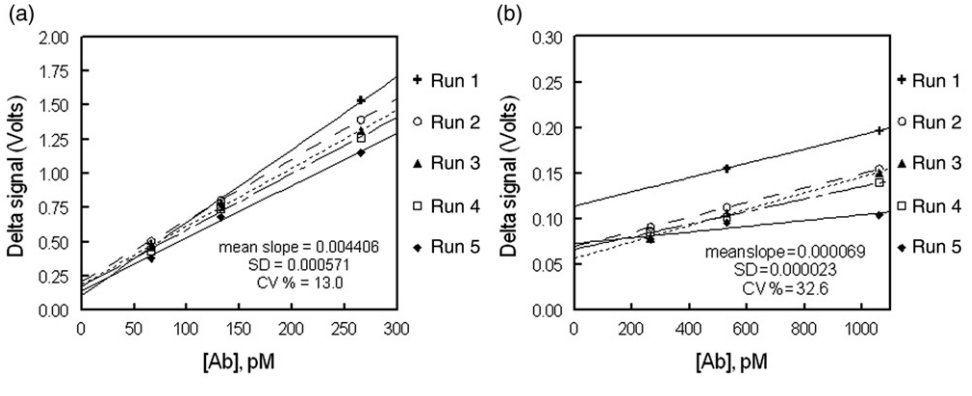

Figure 5. Effect of bead support composition on the reproducibility of antibody dose-response curves. 98 μm diameter beads made of polystyrene (Panel (a)) or polymethylmethacrylate (Panel (b)) were coated with the same caffeine-albumin conjugate and packed into the flow cell of the sensor. Varying concentrations of antibody were allowed to flow over the flow cell and the Delta signal was plotted versus antibody concentration. The slopes of the lines generated in the 5 different runs were analysed for reproducibility.

dose-response curves. Thus, the polystyrene beads were chosen for use with the sensor because they produced more reproducible data with a higher sensitivity for the detection of fluorescently labelled antibody bound to the beads.

3.3 *Analytical performance in the caffeine model system*

The sensor was designed to autonomously analyse water samples drawn in from the exterior port. To determine the sensor's ability to successfully draw and mix samples, calibration curves were constructed. For these experiments, the concentration of labelled anti-caffeine antibody was fixed at 132.5 pM, which provided a delta value of approximately one in the absence of added caffeine. The concentration of caffeine was varied from 0 to 5.0 nM, as shown in Figure 6a. The percent inhibition of the delta values as a function of caffeine concentration are shown as an example of a calibration curve generated by the sensor (circles); the triangles show the CV determined for each point on the curve. The sensor showed acceptable precision, ~15% for all caffeine concentrations. The minimal level of detection (MDL) for each experiment was determined by calculating the mean and SD for the delta values obtained from samples without caffeine. The SD was multiplied by 2, and subtracted from the mean value. The caffeine concentration that corresponded to this 0–2SD calculated delta (60 pM) was determined from the curve to be the MDL.

To determine the reliability of the estimation of caffeine in an unknown sample, spike and recovery experiments were performed. A predetermined concentration of caffeine was spiked into buffer and then the concentration of the sample recovered was estimated using a calibration curve similar to that shown in Figure 6a. The results from these spike and recovery experiments are summarised in Table 1. The sensor showed good correlation, less than 20% difference, between the actual and estimated amounts of caffeine present in the linear portion of the calibration curve, where the caffeine concentration was 1.0 nM or lower. When the caffeine concentration in the sample was greater than 1.0 nM, the estimated concentration from the calibration curve was ~60% of the actual concentration.

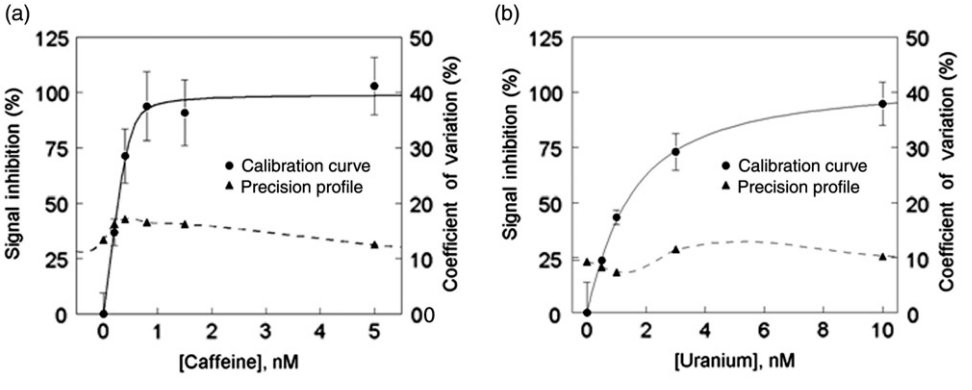

Figure 6. Calibration curves and precision profiles developed using the underwater sensor; (a) calibration curve (circles) and coefficient of variation (triangles) for analysis of the model analyte, caffeine; (b) calibration curve (circles) and coefficient of variation (triangles) for analysis of hexavalent uranium. The plotted points on the calibration curves represent the mean ± SD ($n = 3$).

Table 1. Analytical recovery of spiked samples.

Added (nM)	Found (nM)	Recovery (%)
Caffeine		
0.2	0.193 ± 0.033	96.4 ± 16.5
0.4	0.419 ± 0.096	104.7 ± 24.0
0.8	0.930 ± 0.133	116.3 ± 16.6
2.5	1.570 ± 0.074	62.8 ± 3.0
Uranium		
0.5	0.455 ± 0.145	91.0 ± 29.0
1.0	1.050 ± 0.160	105.0 ± 16.0
3.0	3.126 ± 0.375	104.2 ± 12.5
10	9.605 ± 0.378	96.1 ± 3.8

Practically, this means that the immunosensor is able to provide a yes/no answer for analyte presence upon initial analysis. In situations where more detailed information is necessary, the sample could be analysed at several different dilutions in order to more accurately determine the concentration of analyte.

3.4 *Environmental uranium*

The calibration curve generated for determination of uranium concentration is shown in Figure 6b, along with the precision profile. Again the precision was good with the CV below 15% at each uranium concentration. Table 1 indicates that the spike and recovery data is similar for both uranium and caffeine, demonstrating the ease with which this sensor can be adapted for different analytes.

To demonstrate that the sensor could be used to detect contaminants in environmental samples, groundwater containing U(VI) was also analysed. These samples were collected in the summer of 2008 in Rifle, CO during a field bioremediation experiment [46]. The samples had been collected from a single monitoring well at various times after beginning remediation; they were stabilised by the addition of acid and subsequently stored at 4°C. The U(VI) content of the samples was determined by an independent contractor using Kinetic Phosphorescence Analysis (KPA) [50,51]. A comparison of the uranium concentration determined using the immunosensor to that obtained by KPA is shown in Figure 7. Like the KPA, the immunosensor was able to detect changes in uranium during the bioremediation experiment. With the exception of the sample with the highest uranium concentration (the 7/22 sample), the U(VI) concentrations determined by the two techniques were within experimental error. The sample collected on 7/22 had a concentration of U(VI) that placed it outside of the linear range of the immunosensor ($\sim$0.25–1.5 nM). For best precision, such samples should be reanalysed at a higher dilution.

The MDL in the assay was 241 pM; since samples were analysed at a dilution of 1:400, the sample MDL was 96.4 nM, which is well below the EPA action limit of 126 nM or 30 ppb. As with the caffeine model system, the immunosensor was able to quickly provide data on the presence of uranium and allowed the capability of reanalysis at another dilution for more accurate data, if necessary, while still in the field.

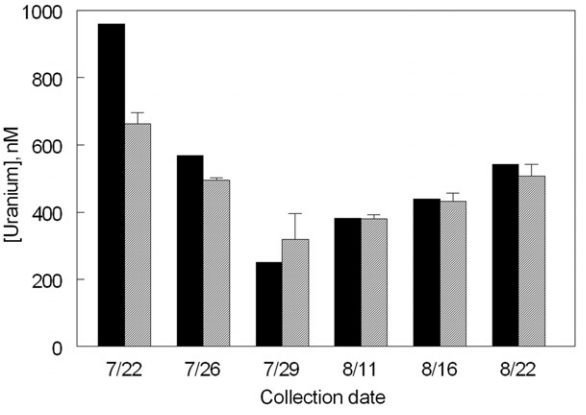

Figure 7. Comparison of KPA (solid bars) and immunosensor (hatched bars) analysis of groundwater samples contaminated with uranium. The groundwater samples were collected from a single well on the dates indicated. The immunosensor analysed the groundwater samples at a final dilution of 1 : 400. Data is reported as the mean ± SD ($n = 3$).

4. Conclusion

A novel immunosensor has been designed to operate underwater by autonomously drawing and analysing samples. The programming features of the sensor are sufficiently flexible to allow analysis by at least 2 different modes of operation. For the caffeine experiments, the sample bags were loaded with the caffeine standards and the sensor autonomously mixed the assay solutions required for the calibration curve; unknown samples were drawn through the nose inlet directly into the draw syringe for immediate analysis. For the uranium experiments, the assay mixtures required for the calibration curve were prepared by the operator, and the calibration curve was generated before analysis of the unknowns. The unknowns were drawn from the nose inlet into the sample bags; these unknowns were then autonomously analysed. This second mode of operation may be preferable when it is necessary to collect samples over shorter time intervals. In this mode of operation, the sensor could draw an environmental sample, store it in a sample bag and perform the analysis while being moved to another sampling location. The environmental sample remaining in the sample bag would then be available for further testing while still in the field or back at the laboratory. This mode of operation would also permit the stored samples to be analysed for other contaminants or for parameters such as salinity or pH.

The versatility of the immunosensor is also apparent in the ease of reconfiguring the sensor for the analysis of a different analyte. The interchangeable flow cells and reagent bags make switching analyte detection simple, even in a non laboratory setting. Although these initial experiments utilised caffeine as the model analyte, the sensor could be adapted to detect many other small molecular weight environmental contaminants, including the U(VI) used as the second example presented herein. The sensor was also able to accept antibodies labelled by two different methods. The caffeine assay utilised an antibody that was covalently conjugated to the fluorophore, while 12F6, the anti-uranium antibody, relied on a secondary labelled Fab for detection. The use of a labelled Fab increases the variety of analytes that can be assessed, since not all antibodies respond well to the covalent attachment of a fluorophore. Both model systems showed comparable levels

of precision. The difference in the MDLs for the two model systems was a function of the each antibody's affinity, not a reflection of the mode of labeling or the sensor platform [45,52].

In this report we have demonstrated that the immunosensor is able to operate with the accuracy and precision necessary to estimate concentrations of two distinct unknown analytes. These data confirm the sensor's ability to analyse a potentially wide variety of contaminants in hazardous or otherwise inaccessible settings where it is inadvisable to send a human.

Acknowledgements

This research was supported by Grant #N00014-06-1-1136 from the United States Office of Naval Research to the Tulane/Xavier Center for Bioenvironmental Research (D.A.B., PI of sensor subproject). Additional support was provided by the Tulane Phase II Katrina Fund. The authors thank Sara A. Morris of S.M. Stoller Corporation, Grand Junction, CO for providing the KPA analysis of Rifle groundwater samples and Terrance Lackie of Sapidyne Instruments for his assistance in sensor development.

References

[1] U.S. Department of Energy, Office of Environmental Management. http://www.em.doe.gov/Pages/EMHome.aspx
[2] Food and Agriculture Organization of the United Nations, *Marine Biotoxins* (2004).
[3] U.S. Office of Naval Research. Naval S&T Strategic Plan (2007). http://www.onr.navy.mil/about/docs/0703_naval_st_strategy.pdf
[4] S. Diercks, K. Metfies, and L.K. Medlin, Biosens. Bioeletron. **23**, 1527 (2008).
[5] M. Gray, B. Warwrik, J. Paul, and E. Casper, Appl. Environ. Microbiol. **69**, 5726 (2003).
[6] K. Metfies, S. Huljic, M. Lange, and L.K. Medlin, Biosens. Bioeletron. **20**, 1349 (2005).
[7] A.J. Baeumner, R.N. Cohen, V. Miksic, and J. Min, Biosens. Bioeletron. **18**, 405 (2003).
[8] E.A. Barlaan, S. Furukawa, and K. Takeuchi, Environ. Microbiol. **9**, 690 (2007).
[9] C.W. Price, D.C. Leslie, and J.P. Landers, Lab. Chip. **9**, 2484 (2009).
[10] E.J. Cho, J.W. Lee, and A.D. Ellington, Annu. Rev. Anal. Chem. **2**, 241 (2009).
[11] S. Tombelli and M. Mascini, Curr. Opin. Mol. Ther. **11**, 179 (2009).
[12] T.M. Lerga and C.K. O'Sullivan, Anal. Chim. Acta. **610**, 105 (2008).
[13] Z. Jiang, Y. Fan, M. Chen, A. Liang, X. Liao, G. Wen, X. Shen, X. He, H. Pan, and H. Jiang, Anal. Chem. **81**, 5439 (2009).
[14] L. Cao, H. Lin, and V.M. Mirsky, Anal. Chim. Acta **589**, 1 (2007).
[15] D. Mazumdar, J. Liu, and Y. Lu, Nanotechnol. Appl. Clean Water 427 (2009).
[16] M. Rodriguez Jr, C.A. Sanders, and E. Greenbaum, Biosens. Bioeletron. **17**, 843 (2002).
[17] B.M. Phillips, B.S. Anderson, J.W. Hunt, P.A. Nicely, R.A. Kosaka, R.S. Tjeerdema, V. de Vlaming, and N. Richards, Environ. Toxicol. Chem. **22**, 435 (2004).
[18] D.G. Varsamis, E. Touloupakis, P. Morlacchi, D.F. Ghanotakis, M.T. Giardi, and D.C. Cullen, Talanta **77**, 42 (2008).
[19] F.F. Roberto, J.M. Barnes, and D.F. Bruhn, Talanta **58**, 181 (2002).
[20] D.G. Heijerick, C.R. Janssen, C. Karlen, I. Odnevall Wallinder, and C. Leygraf, Chemosphere **47**, 1073 (2002).
[21] M. Bouzid, D. Steverding, and K.M. Tyler, Curr. Opin. Biotechnol. **19**, 302 (2008).
[22] B. Khadro, P. Namour, F. Bessueille, D. Leonard, and N. Jaffrezic-Renault, J. Environ. Sci. (China) **21**, 545 (2009).

[23] W. Xuejiang, S.V. Dzyadevych, J.M. Chovelon, N. Jaffrezic Renault, C. Ling, X. Siqing, and Z. Jianfu, Talanta **69**, 450 (2006).
[24] C. Lei, M.M. Valenta, K.P. Saripalli, and E.J. Ackerman, J. Environ. Qual. **36**, 233 (2007).
[25] M. Campas and J.L. Marty, Anal. Chim. Acta **605**, 87 (2007).
[26] W. Schuhmann, J. Biotechnol. **82**, 425 (2002).
[27] M. Campas, B. Prieto-Simon, and J.L. Marty, Semin. Cell Dev. Biol. **20**, 3 (2009).
[28] J.A. Ho, L.C. Wu, M.R. Huang, Y.J. Lin, A.J. Baeumner, and R.A. Durst, Anal. Chem. **79**, 246 (2007).
[29] S.R. Hong, S.J. Choi, H.D. Jeong, and S. Hong, Biosens. Bioelectron. **24**, 1635 (2009).
[30] C.S. Theegala, D.D. Small, and W.T. Monroe, J. Environ. Sci. Health A Tox. Hazard Subst. Environ. Eng. **43**, 478 (2008).
[31] S.D. Leskinen, V.J. Harwood, and D.V. Lim, J. Water Health **7**, 674 (2009).
[32] F. Long, H.C. Shi, M. He, and A.N. Zhu, Biosens. Bioelectron. **23**, 1361 (2008).
[33] E. Mauriz, A. Calle, A. Montoya, and L.M. Lechuga, Talanta **69**, 359 (2006).
[34] J. Tschmelak, G. Proll, and G. Gauglitz, Talanta **65**, 313 (2005).
[35] E.S. Bromage, G.G. Vadas, E. Harvey, M.A. Unger, and S.L. Kaattari, Environ. Sci. Technol. **41**, 7067 (2007).
[36] H. Yu, R.M. Jones, and D.A. Blake, Intern. J. Environ. Anal. Chem. **85**, 817 (2005).
[37] R. Siegener and R.F. Chen, Mar. Pollut. Bull. **44**, 383 (2002).
[38] I.J. Buerge, T. Poiger, M.D. Muller, and H.R. Buser, Environ. Sci. Technol. **37**, 691 (2003).
[39] S.T Glassmeyer, E.T. Furlong, D.W. Kolpin, J.D. Cahill, S.D Zaugg, S.L. Werner, M.T. Meyer, and D.D. Kryak, Environ Sci. Technol. **39**, 5157 (2005).
[40] R.H. Meade, editor, *Contaminants in the Mississippi River* (U.S. Geological Survey, Reston, VA, 1995).
[41] D.W. Kolpin, E.T. Furlong, M.T. Meyer, E.M. Thurman, S.D. Zaugg, L.B. Barber, and H.T. Buxton, Environ. Sci. Technol. **36**, 1202 (2002).
[42] H.A. Vrionis, R.T. Anderson, I. Ortiz-Bernad, K.R. O'Neill, C.T. Resch, A.D. Peacock, R. Dayvault, K. Karp, D.C. White, P.E. Long, and D.R. Lovley, Appl. Environ. Microbiol. **71**, 6308 (2005).
[43] R.T. Anderson, H.A. Vrionis, I. Ortiz-Bernad, C.T. Resch, P.E. Long, R. Dayvault, K. Karp, S. Marutzky, D.R. Metzler, A. Peacock, D.C. White, M. Lowe, and D.R. Lovley, Appl. Environ. Microbiol. **69**, 5884 (2003).
[44] A.L. N'Guessan, H.A. Vrionis, C.T. Resch, P.E. Long, and D.R. Lovley, Environ. Sci. Technol. **42**, 2999 (2008).
[45] R.C. Blake 2nd, A.R. Pavlov, M. Khosraviani, H.E. Ensley, G.E. Kiefer, H. Yu, X. Li, and D.A. Blake, Bioconjug. Chem. **15**, 1125 (2004).
[46] S.J. Melton, H. Yu, K.H. Williams, S.A. Morris, P.E. Long, and D.A. Blake, Environ. Sci. Technol. **43**, 6703 (2009).
[47] R.C. Blake II, A.R. Pavlov, and D.A. Blake, Anal. Biochem. **272**, 123 (1999).
[48] D.A. Blake, P. Chakrabarti, M. Khosraviani, F.M. Hatcher, C.M. Westhoff, P. Goebel, D.E. Wylie, and R.C. Blake II, J. Biol. Chem. **271**, 27677 (1996).
[49] R.C. Blake II and D.A. Blake, Met. Mol. Biol. **248**, 417 (2004).
[50] R. Brina and A.G. Miller, Spectroscopy **8**, 830 (1993).
[51] R. Brina, Am. Environ. Lab **7**, 16 (1995).
[52] D.A. Blake, H. Yu, E.A. James, X. Li, and R.C. Blake, in *Uranium in the Environment: Mining Impact and Consequences*, edited by B.J. Merkel and A. Hasche-Berger (Springer-Verlag, Berlin, 2006).